DALTON
FULL PAPER

Synthesis and properties of iron-group hydrido-cyano complexes *trans*-[MH(CN)$(L)_2$], M = Fe, Ru or Os, L = diphosphine, and their hydrogen, trifluoroboron and triphenylboron isocyanide derivatives of the type *trans*-[MH(CNH)$(L)_2$]O_3SCF_3, *trans*-[MH$(CNBX_3)(L)_2$], X = F or Ph, and *trans*-[M$(H_2)(CNBF_3)$-$(dppp)_2$]BF_4 [dppp = $Ph_2P(CH_2)_3PPh_2$]

Eliana Rocchini,[a] Pierluigi Rigo,*[a] Antonio Mezzetti,[ab] Tim Stephan,[c] Robert H. Morris,*[c] Alan J. Lough,[c] Cameron E. Forde,[c] Tina P. Fong[c] and Samantha D. Drouin[c]

[a] *Dip. di Scienze e Tecnol. Chimiche, Università di Udine, Via del Cotonificio 108, I-33100 Udine, Italy*
[b] *Laboratorium für Anorganische Chemie, ETH-Zentrum, Universitätstrasse 16, CH-8092 Zürich, Switzerland*
[c] *Department of Chemistry, University of Toronto, 80 St. George St., Toronto, Ontario, M5S 3H6, Canada*

Received 30th June 2000, Accepted 1st September 2000
First published as an Advance Article on the web 2nd October 2000

Complexes *trans*-[MH(CN)L_2] **1** {L = $PPh_2(CH_2)_nPPh_2$, *n* = 1 (dppm), 2 (dppe) or 3 (dppp), and $PR_2CH_2CH_2PR_2$, R = Et (depe) or *para*-tolyl (dtpe), M = Fe (for dppe, depe and dtpe only), Ru or Os} were prepared by displacing with cyanide the halide from *trans*-[MH(X)L_2], X = Br or Cl, or dihydrogen from *trans*-[Ru(H_2)H$(dppe)_2$]BPh_4. Systematic trends in the IR and ^{1}H, ^{31}P and ^{13}C NMR and electrochemical properties are noted. The addition of one equivalent of HOTf (HO_3SCF_3) or [$HPPh_3$]OTf to *trans*-[MH(CN)L_2] **1** with *n* = 1, 2 or 3 usually produces the hydrogen isocyanide complexes *trans*-[MH(CNH)L_2]OTf **2**. The use of $^{13}CN^-$ or $C^{15}N^-$ in compounds **1** provides evidence for the MCNH coordination mode over MNCH. Protonation at the M–H bond to give dihydrogen complexes *trans*-[M(H_2)(CN)L_2]$^+$ occurs to a small degree for M = Ru, *n* = 1 or 3, in CH_2Cl_2 and completely for M = Os, L = depe. The use of HBF_4·Et_2O results in a variety of products including *trans*-[MH(CNH)L_2]BF_4 **2***, *trans*-[MH$(CNBF_3)L_2$] and *trans*-[M$(H_2)(CNBF_3)L_2$]$^+$. The dihydrogen ligand in the last compound with M = Ru, L = dppp, is readily replaced by η^1-BF_4^-. Structures of the compounds **2** (M = Ru, L = dppe), *trans*-[RuH$(CNBF_3)(dppe)_2$] and **2*** (M = Os, L = dppe) are reported. The CNH ligand is a good hydrogen-bond donor so that NH · · · O or NH · · · F hydrogen bonds with the counter ion are formed. The reaction of BPh_4^- with the CNH ligand of **2** (M = Ru, L = dppe) produces *trans*-[Ru(H)$(CNBPh_3)(dppe)_2$], the structure of which is reported. Therefore the CNH ligand reacts readily with BX_4^- (X = F or Ph) to produce $CNBX_3^-$ ligands and HX.

Introduction

The coordination chemistry and reactivity of the cyanide ligand have been studied for many years. The attack of electrophiles on cyanide ligands (NC[M], [M] = metal and ancillary ligands) can produce hydrogen isocyanide (HNC[M]$^+$),[1–8] aminocarbene (H_2NC[M]$^+$),[9] organoisocyanides (RNC[M]$^+$),[10–12] boron-containing (X_3BNC[M])[7,8,13–15] or bridged metal ([M′]NC[M])[16] complexes for example. The protonation of cyanide coordinated at the active site of nitrogenase is likely to be a step in its reduction to methane and ammonia, a process that is catalysed by this enzymatic system.[17] There has been a resurgence of interest in cyanide as a ligand in biology with the discovery that nickel–iron and iron-only hydrogenases have active sites containing Fe–CN groups.[18–21] Alkyl isocyanides have a vast chemistry of their own while cyano-bridged bimetallic and polymetallic complexes are of particular interest in electron-transfer processes and materials chemistry.[16] In materials science there continues to be much interest in the assembly of complex structures starting with squares and cubes with MCNM′ edges[22] and continuing to larger assemblies with, for example, useful magnetic properties.[23] The chemistry of the $CNBPh_3^-$ ligand is thought to be particularly important in the industrial hydrocyanation of butadiene to produce adiponitrile, a process catalysed by nickel phosphite complexes promoted with BPh_3.[24]

We have shown that cyanide and hydrogen isocyanide ligands promote the formation of dihydrogen ligands on d^6 Fe^{II}, Ru^{II} and Os^{II}.[2–5] Thus when the complex *trans*-[FeH(CN)$(depe)_2$] **1Fe4** (see Table 1 for the numbering scheme) is protonated with 1 or 2 equivalents of HBF_4·Et_2O under specific conditions the products are monocationic or dicationic dihydrogen complexes *trans*-[Fe(H_2)(CN)$(depe)_2$]$^+$, **3Fe4**, and *trans*-[Fe(H_2)(CNH)-$(depe)_2$]$^{2+}$, **4Fe4**, respectively. The use of different acids (*e.g.* HOTf = HO_3SCF_3), ligands, and metal ions in complexes **1M*j*** can lead to the formation of hydrogen isocyanide complexes **2M*j*** or dihydrogen complexes **3M*j*** or an equilibrium mixture of products (Scheme 1). The properties of the dihydrogen complexes have been described in detail.[5] In the present work we describe the synthesis and periodic properties of the starting cyanide complexes **1M*j*** and hydrido(hydrogen isocyanide) complexes **2M*j***. In addition we study the reaction of the CNH ligand with a boron–fluorine bond of BF_4^- or a boron–carbon bond of BPh_4^- to produce $CNBX_3^-$ ligands.

Table 1 The numbering scheme for the complexes ***i*M*j***

i*M*j	***i***	**M**	***j***	L	Abbrev.
$[MH(CN)L_2]$	**1**	Fe	**1**	$PPh_2CH_2PPh_2$	dppm
$[MH(CNH)L_2]OTf$	**2**	Ru	**2**	$PPh_2(CH_2)_2PPh_2$	dppe
$[M(H_2)(CN)L_2]OTf$	**3**	Os	**3**	$PPh_2(CH_2)_3PPh_2$	dppp
$[M(H_2)(CNH)L_2][OTf]_2$	**4**		**4**	$PEt_2(CH_2)_2PEt_2$	depe
$[MH(CNBF_3)L_2]$	**5**		**5**	$\{P(C_6H_4Me\text{-}4)_2CH_2\}_2$	dtpe
$[MH(CNBPh_3)L_2]$	**6**				
$[M(H_2)(CNBF_3)L_2]OTf$	**7**				
$[M(BF_4)(CNBF_3)L_2]$	**8**				
Other salts	***i***				
$[MH(CNH)L_2]BF_4$	**2***				
$[M(H_2)(CN)L_2]BF_4$	**3***				
$[M(H_2)(CNH)L_2][BF_4]_2$	**4***				
$[M(H_2)(CNBF_3)L_2]BF_4$	**7***				

Table 2 Analytical and IR spectroscopic data

Complex	Colour	Yield (%)	Analysis[a] (%)			IR/cm^{-1}	
			C	H	N	*ν*(MH)	*ν*(CN)
1Ru1 *trans*-$[RuH(CN)(dppm)_2]$	White-cream	96	67.66(68.30)	5.06(5.06)	1.54(1.56)	1844w	2079s
1Os1 *trans*-$[OsH(CN)(dppm)_2]$	White	85	62.44(62.12)	4.62(4.60)	1.41(1.42)	1903w	2076s
1Fe2 *trans*-$[FeH(CN)(dppe)_2]$	Orange	89	72.50(72.36)	5.79(5.61)	1.38(1.59)	1787w	2058s
1Ru2 *trans*-$[RuH(CN)(dppe)_2]$	White	94	68.70(68.82)	5.47(5.34)	1.51(1.51)	1836m	2078s
1Os2 *trans*-$[OsH(CN)(dppe)_2]$	White	80	62.52(62.77)	4.94(4.87)	1.32(1.38)	1907m	2073s
1Ru3 *trans*-$[RuH(CN)(dppp)_2]$	White	73	71.22(71.06)	5.84(5.77)	1.04(1.36)	1789w	2069s
1Os3 *trans*-$[OsH(CN)(dppp)_2]$	White	70	66.30(67.15)	5.54(5.47)	1.17(1.17)	1881w	2064s
1Fe4 *trans*-$[FeH(CN)(depe)_2]$	Yellow	94	50.98(50.92)	10.54(9.97)	3.19(2.83)		2056, 2043s
1Ru4 *trans*-$[RuH(CN)(depe)_2]$	Yellow	94	46.96(46.66)	9.46(9.14)	2.52(2.59)	1812m	2074s
1Os4 *trans*-$[OsH(CN)(depe)_2]$	White	80				1896m	2071s
1Fe5 *trans*-$[FeH(CN)(dtpe)_2]$	Yellow	60	73.80(73.86)	6.62(6.61)	1.35(1.41)		2056s
2Ru1 *trans*-$[RuH(CNH)(dppm)_2]OTf$	White	84	59.42(59.66)	4.41(4.43)	1.33(1.34)	1832w	2021w
2Os1 *trans*-$[OsH(CNH)(dppm)_2]OTf$	Green	82	54.75(54.98)	4.07(4.08)	1.23(1.23)	2019w	2078w
2Fe2 *trans*-$[FeH(CNH)(dppe)_2]OTf$	Yellow	>90	62.80(62.98)	5.13(4.89)	1.74(1.36)	1802w	2052s
2Ru2 *trans*-$[RuH(CNH)(dppe)_2]OTf$	White	97	60.64(60.33)	4.69(4.65)	1.29(1.30)		(2500w)[b]
2Os2 *trans*-$[OsH(CNH)(dppe)_2]OTf$	White	50	55.46(55.71)	4.50(4.33)	1.43(1.20)		2022s
2Ru3 *trans*-$[RuH(CNH)(dppp)_2]OTf$	Yellow	82	59.67(60.98)	4.98(4.93)	1.24(1.27)	2000w	2069w
2Os3 *trans*-$[OsH(CNH)(dppp)_2]OTf$	Pink	85	57.49(57.37)	5.07(4.98)	1.13(1.13)	1917w	2070s
5Ru2 *trans*-$[RuH(CNBF_3)(dppe)_2]$	White	86	63.75(64.12)	5.15(4.97)	1.39(1.41)	1874w	2140s
5Ru3 *trans*-$[RuH(CNBF_3)(dppp)_2]$	White	94	62.25(64.71)	5.15(5.23)	1.33(1.37)	1967w	2121vs
5Os3 *trans*-$[OsH(CNBF_3)(dppp)_2]$	White	90	58.65(59.52)	4.80(4.81)	1.24(1.26)	1962w	2110vs
6Ru2 *trans*-$[RuH(CNBPh_3)(dppe)_2]$	White	87	69.22(69.13)	5.26(5.31)	0.86(1.12)		2124s
7*Ru3 *trans*-$[Ru(H_2)(CNBF_3)(dppp)_2]BF_4$	White	77	56.95(59.59)	5.03(4.91)	1.20(1.26)		2174vs
7*Os3 *trans*-$[Os(H_2)(CNBF_3)(dppp)_2]BF_4$	White	75	54.98(55.15)	4.61(4.54)	1.17(1.17)		2174vs
8Ru3 *trans*-$[Ru(FBF_3)(CNBF_3)(dppp)_2]$	White	90	59.11(59.70)	4.70(4.74)	1.26(1.27)		2126s

[a] Calculated values in parentheses. [b] O · · · HNCRuH combination mode. **2Ru2-d** gives a stronger broad band at 2277 cm^{-1}.

Results and discussion

Synthesis and properties of the complexes *trans*-$[MH(CN)L_2]$ 1M*j*

The synthesis of the complexes **1Ru1**, **1Os1**, **1Fe2**, **1Os2**, **1Ru3**, **1Os3**, **1M4**, M = Fe, Ru or Os, **1Fe5** (see Table 1 for the numbering scheme) involves metathesis of the halide in *trans*-$[MH(X)L_2]$ (X = Br or Cl) for cyanide from KCN or NaCN in MeOH, CH_2Cl_2–MeOH–water or THF–MeOH. Owing to the ease of synthesis of *trans*-$[RuH(\eta^2\text{-}H_2)(dppe)_2]BPh_4$, the complex *trans*-$[RuH(CN)(dppe)_2]$ **1Ru2** is made by displacement of H_2 by cyanide from KCN. The iron complexes are yellow while the ruthenium and osmium complexes are colourless apart from **1Ru4** which is yellow. They have been characterized by microanalysis and IR spectroscopy (Table 2) and by NMR (Tables 3, 4). Some properties of the compounds **1Fe2**[25] and **1Ru4**[26] that have already been reported are in agreement with our measurements.

The M–H stretching wavenumbers are found in the region 1910–1785 cm^{-1}, the CN stretching frequencies in the 2100–2000 cm^{-1} region. The *ν*(MH) mode is observed to increase in frequency on going from Fe to Ru ($\Delta\nu$ 49 cm^{-1}) and from Ru to Os ($\Delta\nu$ 60–90 cm^{-1}), indicating that the M–H bond strength increases as M changes from Fe to Ru to Os. A similar trend was observed for the complexes *trans*-$[MH(CN)(dmpe)_2]$.[27] The observed trend for the *ν*(CN) mode is a decrease in frequency on going from Ru ≥ Os ≥ Fe due in part to increased M–CN π-back bonding, thus weakening the CN bond. The *ν*(CN) stretching frequency also decreases as the diphosphine ligand is changed from dppm > dppe > depe > dppp. In this series, two factors contribute to the raising in energy of the metal d_π orbitals that form π bonds with the cyanide ligand: (1) an increase in basicity of the diphosphine with constant bite angle (dppe < depe); (2) an increase in bite angle with fairly constant basicity (dppm < dppe < dppp).

Table 3 ^{1}H, ^{31}P-{^{1}H} and ^{19}F-{^{1}H} NMR spectroscopic data[a,b] for the cyanide complexes

Complex	^{1}H	^{31}P-{^{1}H}	^{19}F-{^{1}H}
1Ru1	7.7–6.9 (m, PC_6H_5), 4.7 (br, 4 H, PCH_2), −7.4 (q, 1 H, RuH, ^{2}J(HP) = 20.2)[c]	3.0 (br s)[d]	
1Os1	7.7–7.0 (m, PC_6H_5), 5.5 (br, 4 H, PCH_2), −8.7 (q, 1 H, OsH, ^{2}J(HP) = 17.1)[c]	−44.4 (br s)[d]	
1Fe2	7.9–6.8 (m, PC_6H_5), 2.7 (br, 4 H, PCH_2), 2.19 (br, 4 H, PCH_2), −14.9 (q, 1 H, FeH, ^{2}J(HP) = 45)[e,f]	90.9 (s)[e,g]	
1Ru2	6.8–7.8 (m, 40 H, PC_6H_5), 2.0–2.5 (m, 8 H, PCH_2CH_2P), −10.6 (q, 1 H, RuH, ^{2}J(HP) = 19.6)[e,f]	68.9 (s)[e,g]	
1Os2	6.8–7.7 (m, 40 H, PC_6H_5), 1.9–2.6 (m, 8 H, PCH_2CH_2P), −11.8 (q, 1 H, OsH, ^{2}J(HP) = 17.4)[e,f]	33.3 (s)[e,g]	
1Ru3	7.7–6.9 (m, 40 H, PC_6H_5), 2.5 (br, 4 H, PCH_2), 2.2 (br, 4 H, PCH_2), 1.4 (br, 4 H, PCH_2CH_2), −9.1 (q, 1 H, RuH, ^{2}J(HP) = 20.2); T = 173 K, −9.0 (tt, 1 H, RuH, ^{2}J(HP) = 26.3, ^{2}J(HP′) = 13.2)[c]	22.7 (s); T = 173 K, 17.2 (t), 27.3 (t, J(PP′) = 40.7)[d]	
1Os3	7.6–6.9 (m, PC_6H_5), 2.8 (br, 4 H, PCH_2), 2.4 (br, 4 H, PCH_2), 1.4 (br, 4 H, PCH_2CH_2), −10.4 (q, 1 H, OsH, ^{2}J(HP) = 17.7); T = 173 K, −10.4 (tt, 1 H, OsH, ^{2}J(HP) = 22.5, ^{2}J(HP′) = 11.3)[c]	−20.4 (br); T = 173 K, −24.6 (t), −15.5 (t, ^{2}J(PP′) = 28.9)[d]	
1Fe4	2.4 (br, 4 H, PCH_2), 1.6 (br, 8 H, CH_2CH_3), 1.2 (br, 4 H, PCH_2), 1.0 (br, 24 H, CH_2CH_3), 0.9 (br, 8 H, CH_2CH_3), −17.3 (q, 1 H, FeH, ^{2}J(HP) = 45)[e,f]	93.5 (s)[e,g]	
1Ru4	1.7–2.4 (m, 8 H, PCH_2CH_2P), 1.3–1.6 (m, 16 H, CH_2CH_3), 0.8–1.2 (m, 24 H, CH_2CH_3), −12.6 (q, 1 H, RuH, ^{2}J(HP) = 20.3)[e,f]	67.3 (s)[e,g]	
1Os4	0.8–2.6 (m, 48 H, $(CH_3CH_2)_2PCH_2CH_2P(CH_3CH_2)_2$), −14.0 (q, 1 H, OsH, ^{2}J(HP) = 17.4)[e,f]	30.6 (s)[e,g]	
1Fe5	−15.1 (q, 1 H, FeH, ^{2}J(HP) = 44)[e]	89 (s)	
2Ru1	7.7–6.8 (m, PC_6H_5), 4.9 (br, 2 H, PCH_2), 4.6 (br, 2 H, PCH_2), −5.6 (q, 1 H, RuH, ^{2}J(HP) = 20.2); T = 193 K, 9.5 (br s, 1 H, CNH), −5.7 (q, 1 H, RuH, ^{2}J(HP) = 19.9)[c]	1.2 (br s); T = 193 K, 0.4 (br s)[d]	
2Os1	8.0–6.2 (m, PC_6H_5), 5.4 (br, 4 H, PCH_2), −6.6 (q, 1 H, OsH, J(PH) = 18.4)[c]	−44.4 (br s)[d]	
2Fe2	9.8 (t, 1 H, NH, ^{1}J(NH) = 80), 7.4–7.0 (m, 40 H, PC_6H_5), 2.50 (br, 4 H, PCH_2-CH_2P), 2.06 (br, 4 H, PCH_2CH_2P), −10.96 (q, 1 H, FeH, ^{2}J(PH) = 46)[f]	87.4 (s)[g]	
2Ru2	10.2 (t, 1 H, NH, ^{1}J(HN) = 73.3), 6.8–7.8 (m, 40 H, PC_6H_5), 2.2–2.6 (m, 8 H, PCH_2CH_2P), −9.0 (q, 1 H, RuH, ^{2}J(HP) = 19.5)[f]	66.6 (s)[g]	
2Os2	9.9 (td, 1 H, NH, ^{1}J(NH) = 81.5), 6.9–7.4 (m, 40 H, PC_6H_5), 2.35 (m, 8 H, PCH_2CH_2P), −10.0 (qd, 1 H, OsH)[f]	32.0 (d), ^{2}J(POs) = 181.4[g]	
2Ru3	7.6–7.0 (m, PC_6H_5), 2.3 (br, 8 H, PCH_2), 1.4 (br, 4 H, PCH_2CH_2), −7.2 (q, 1 H, RuH, ^{2}J(HP) = 20.4)[c]	20.0 (br); T = 193 K, 16.1 (t), 23.5 (t, ^{2}J(PP′) = 37.5)[d]	
2Os3	7.6–7.0 (m, PC_6H_5), 2.6 (br, 8 H, PCH_2), 1.5 (br, 4 H, PCH_2CH_2), −8.4 (q, 1 H, RuH, ^{2}J(HP) = 18.7)[c]	−21.6 (br); T = 183 K, −24.5 (t), −18.4 (t, ^{2}J(PP′) = 27.0)[d]	
5Ru2	6.8–7.6 (m, 40 H, PC_6H_5), 2.1–2.6 (m, 8 H, PCH_2CH_2P), −9.6 (q, 1H, RuH, ^{2}J(HP) = 19.4)[f]	67.3 (s)[g]	
5Os2	−10.6 (q, 1 H, OsH, ^{2}J(HP) = 18.2)[f]	32.4 (s)[g]	−145 (br m, BF_3)
5Ru3	7.6–7.0 (m, PC_6H_5), 2.2 (br, 8 H, PCH_2), 1.4 (br, 4 H, PCH_2CH_2), −7.7 (q, 1 H, RuH, ^{2}J(HP) = 20.4)[c]	20.9 (br); T = 193 K, 16.6 (t), 24.5 (t, ^{2}J(PP′) = 38.8)[d]	−147.3 (s, BF_3)[h]
5Os3	7.5–7.0 (m, PC_6H_5), 2.5 (br, 8 H, PCH_2), 1.4 (br, 4 H, PCH_2CH_2), −8.9 (q, 1 H, OsH, ^{2}J(HP) = 18.0)[c]	−21.1 (br); T = 193 K, −24.3 (t), −17.6 (t, ^{2}J(PP′) = 27.0)[d]	−146.9 (s, BF_3)[h]
6Ru2	6.8–7.8 (m, 55 H, C_6H_5), 2.1–2.4 (m, 8 H, PCH_2CH_2P), −11.1 (q, 1 H, RuH, ^{2}J(HP) = 20.7)[f]	66.4 (s)[g]	
7*Ru3	7.6–6.9 (m, PC_6H_5), 2.4 (br, 8 H, PCH_2), 1.7 (br, 4 H, PCH_2CH_2), −4.3 (br, 2 H, RuH_2)[c]	9.1 (br); T = 183 K, 2.7 (t), 15.9 (t, J(PP′) = 28.7)[d]	−152.0 (s, 4 F, BF_4^-), −146.8 (s, 3 F, BF_3)[h]
7*Os3	7.6–6.9 (m, PC_6H_5), 2.6 (br, 8 H, PCH_2), 1.7 (br, 4 H, PCH_2CH_2), −4.7 (br, 2 H, OsH_2)[c]	−29.4 (br); T = 173 K, −36.4 (t), −21.0 (t, J(PP′) = 20.8)[d]	−152.8 (s, 4 F, BF_4^-), −146.6 (s, 3 F, BF_3)[h]
8Ru3	7.6–6.6 (m, PC_6H_5), 2.7 (br, 4 H, PCH_2), 2.4 (br, 4 H, PCH_2), 2.2 (br, 4 H, PCH_2CH_2)[c]	2.8 (br s); T = 183 K, −1.4 (t), 0.7 (t, J(PP′) = 30.0)[d]	−151.3 (s, 4 F, FBF_3), −147.4 (s, 3 F, BF_3)[h]

[a] In CD_2Cl_2 unless otherwise stated (δ, J/Hz); q = quintet. [b] T = 293 K unless otherwise noted. [c] 200 MHz. [d] 81 MHz. [e] C_6D_6. [f] 300 MHz. [g] 120.5 MHz. [h] 188 MHz.

The resonance in the proton NMR spectra due to the hydride ligand of these complexes in CD_2Cl_2 at 20 °C appears at high field as a quintet due to coupling to four equivalent ^{31}P nuclei. At low temperature the patterns of the ^{1}H NMR hydride resonances of **1Ru3** and **1Os3** are triplets of triplets. The inequivalence of pairs of phosphorus nuclei in the dppp complexes is also apparent in the low temperature ^{31}P-{^{1}H} NMR spectra that consist of two triplets. This is common for *trans*-$MXY(dppp)_2$ complexes and probably reflects crowding of adjacent PPh_2 groups and slowing of backbone flipping because of the larger bite angle of this ligand (86–92°) relative to dppe (80–85°) and dppm (71–73°). At room temperature the ^{31}P-{^{1}H} NMR spectra of all of the complexes are singlets. The ^{31}P chemical shifts follow the usual periodic trend Fe > Ru > Os for analogous complexes.

By using $KC^{15}N$ or $K^{13}CN$ the corresponding derivatives *trans*-[RuH($C^{15}N$)$(dppp)_2$] **1Ru3-n** and *trans*-[RuH(^{13}CN)$(dppp)_2$] **1Ru3-c** have also been prepared. The IR spectra of the complexes in Nujol mulls show a ν(CN) absorption at 2039 (**1Ru3-n**) and 2024 (**1Ru3-c**) compared to 2069 cm^{-1} for **1Ru3** (Table 2). The complexes **1Ru3-n** and **1Ru3-c** were used for *in situ* NMR tube preparation of corresponding $C^{15}N$ and ^{13}CN protonation products.

In the ^{1}H NMR spectrum of complex **1Ru3-n** the hydride signal splits into a quintet (^{2}J(H,P) = 20.2 Hz) of doublets (^{3}J(H,^{15}N) = 2.7 Hz). In the case of **1Ru3-c** the ^{31}P signal is a broad doublet (^{2}J(P,C) = 10.3 Hz) while the hydride resonance appears as a quintet (^{2}J(H,P) = 20.1 Hz) of doublets (^{2}J(H,C) = 11.0 Hz). A quintet is also observed for the CN ligand in the proton decoupled ^{13}C NMR spectrum (^{2}J(C,P) = 10.9 Hz) at

Table 4 Additional data for isotopically enriched complexes

Complex	NMR (δ, J/Hz)[a] ν(CN)/cm^{-1}	^{1}H, MH {and NH}	^{31}P-{^{1}H}	^{13}C-{^{1}H} (^{13}CN)	^{19}F
1Fe2-c [FeH(^{13}CN)(dppe)$_2$]	2012		90.9 (d, ^2J(P,C) 17.3)	162.5 (q, ^2J(C,P) 17)	
1Os2-c [OsH(^{13}CN)(dppe)$_2$]	2035		33.3 (d, ^2J(P,C) 8.3)	129.7 (q, ^2J(C,P) 8.3)	
1Ru3-c [RuH(^{13}CN)(dppp)$_2$]	2024	−9.0 (q of d, ^2J(H,P) 20.1, ^2J(H,C) 11.0)	22.7 (br d, ^2J(P,C) 10.3)	156.7 (q, ^2J(C,P) 10.9)	
1Ru3-n [RuH(C^{15}N)(dppp)$_2$]	2039	−9.0 (q of d, ^2J(H,P) 20.2, ^3J(H,N) 2.7)			
1Os3-c [OsH(^{13}CN)(dppp)$_2$]	2021	−10.4 (q of d, ^2J(H,P) 17.6, ^2J(H,C) 4.2)	−20.4 (br d, ^2J(P,C) 6.3)	137.9 (q, ^2J(C,P) 8.1)	
1Os3-n [OsH(C^{15}N)(dppp)$_2$]	2036	−10.4 (q of d, ^2J(H,P) 17.4, ^3J(H,N) 2.4)			
2Os2-c		−10.0 (q of d, ^2J(H,P) 18.3, ^2J(H,C) 7)	32.0 (d, ^2J(P,C) 7.2)		
2Ru3-c	2019[b]	−7.2 (q of d, ^2J(H,P) 20.4, ^2J(H,C) 19.4)	20.0 (br d, ^2J(P,C) 10.3); 16.0, 23.5[c] (A_2X_2, J(P,P′) 38.2, J(P,C) 12.4, J(P′C) 6.6)	165.5 (br q, ^2J(C,P) 10.2)	
2Ru3-n		−7.2 (q of d, ^2J(H,P) 20.5, ^3J(H,N) = 5.5) {10.7[b] (d, ^1J(H,N) 115.7)}			
2Os3-c	2021[d]	−8.2 (q of d, ^2J(H,P) 18.5, ^2J(H,C) 8.7)	−21.7 (br d, ^2J(P,C) 7.1)	153.1 (br)	
2Os3-n		−8.2 (q of d, ^2J(H,P) 18.4, ^3J(H,N) 5.2) {10.4[b] (d, ^1J(H,N) 116.9)}			
5Ru3-c		−7.7 (q of d, ^2J(H,P) 20.3, ^2J(H,C) 15.5)	20.9 (br d, ^2J(P,C) 9.5)	161.4 (br)	−146.9 (br s)
5Os3-c		−8.9 (q of d, ^2J(H,P) 18.0, ^2J(H,C) 7.4)	−21.1 (d, ^2J(P,C) 7.9)	144.5 (br)	−152.0 (s), −146.8 (d, J(F,C) 5.6)
7*Ru3-c		−4.3 (br)	9.1 (br d, ^2J(P,C) 12.7)	147.3 (qd, ^2J(C,P) 13.6, ^3J(C,F) 6.1)	
7*Os3-c		−4.7 (br)	−29.4 (br)	130.4 (br)	−152.8 (s), −146.6 (d, J(F,C) 5.6)

[a] q = quintet. [b] ν(RuH) 1962 cm^{-1}. [c] −90 °C. [d] ν(OsH) 1879 cm^{-1}.

δ 156.7. Similar features are observed for the isotopically labelled forms of **1Os3** (Table 4).

Synthesis and properties of *trans*-[MH(CNH)L$_2$]$^+$

Generally, the addition of one equivalent of HOTf or [HPPh$_3$]OTf to the complexes *trans*-[MH(CN)L$_2$] **1M*j***, j = 1–3, in toluene or diethyl ether produces the hydrogen isocyanide complexes *trans*-[MH(CNH)L$_2$]OTf **2M*j*** (Scheme 1, step i). If these reactions are conducted in CH_2Cl_2 then small amounts of the dihydrogen complexes [Ru(H$_2$)(CN)L$_2$]OTf are also formed in the case of **1Ru1** and **1Ru3** (Scheme 1, step ii) as described elsewhere.[5] The depe complexes **1M4** appear to be protonated completely at the M–H bond (Scheme 1, step ii) to give dihydrogen complexes that are unstable as triflate salts apart from *trans*-[Os(H$_2$)(CN)(depe)$_2$]OTf.[5] There are other ways to prepare these CNH complexes. Triphenylphosphine is used to remove HOTf from the unstable dihydrogen complex **4Ru2** (Scheme 1) to give **2Ru2**; the dihydrogen complex is generated by bubbling H_2 gas into a solution of *trans*-[Ru(OTf)(CNH)(dppe)$_2$]OTf in CH_2Cl_2 (Scheme 1).[5] The unstable dihydrogen complex generated by reaction of *trans*-[Ru(OTf)(CN)(dppe)$_2$] with H_2 rearranges to **2Ru2** (Scheme 1).[5] In certain cases the use of the acids 85% HBF$_4$·Et$_2$O or [HPPh$_3$]BF$_4$ leads to the isolation of analogous salts *trans*-[MH(CNH)L$_2$]BF$_4$ (**2*Fe2**,[2,7] **2*Os2**, **2*Fe5**[2]); otherwise side reactions involving formation of the $CNBF_3^-$ ligand can occur (see below). The complex **2*Fe2** was also obtained in the reaction of NCSiMe$_3$ with [FeH(Cl)(dppe)$_2$], TlBF$_4$ and HBF$_4$.[7]

The molecular structures of complexes **2Ru2** (Fig. 1) and **2*Os2** (Fig. 2) have been determined by use of single crystal X-ray diffraction. The structure of **2*Fe5** has been described briefly.[2] The structures are oriented and labelled in a consistent fashion; for example Figs. 1–4 all show similar conformations in the dppe ligands. The metal–hydride distances increase as Fe–H 1.39(6) < Ru–H 1.53(5) < Os–H 1.70(5) Å (Table 5). The MH(P)$_4$C core bond lengths are almost identical for **2Ru2** and **2*Os2** while those of **2*Fe5** are systematically shorter. The C–N bond of **2*Fe5** (1.183(8) Å) is slightly longer than those of **2Ru2** (1.161(5) Å) and **2*Os2** (1.162(8) Å). The last two are comparable to the C–N distance in [RuCp(PPh$_3$)$_2$(CNH···OTf)].[28] The Ru–C bond in the RuCNH fragment of the latter compound is shorter, 1.930(4), than that of **2Ru2**, 1.998(4) Å, because of the lower *trans* influence of Cp *versus* hydride. The angles H(1M)–M(1)–C(5) and N(1)–C(5)–M(1) in each complex are consistent with a fairly linear HMCNH geometry (see Table 5); linearity is forced by crystal symmetry in the case of **2*Fe5**. The phosphorus atoms bend away from the CNH ligand toward the hydride in each complex with an average C(5)–M–P angle of 94.5 (Fe), 93.7 (Ru) and 93.3° (Os). Despite wide variations in the individual C(5)–M–P angles, the M–P distances in each complex do not vary much. Comparing complex

Scheme 1

Table 5 Selected bond lengths (Å) and angles (°) for complexes **2*Fe5**,[a] **2Ru2**, **2*Os2**, **5Ru2**·CH_2Cl_2, **6Ru2**·CH_2Cl_2 and **6Fe2**[b]

	2*Fe5[a]	2Ru2	2*Os2	5Ru2	6Fe2[b]	6Ru2
M(1)–H(1M)	1.39(6)	1.53(5)	1.70(5)	1.67(3)	1.37(3)	1.61(2)
M(1)–C(5)	1.842(6)	1.998(4)	1.983(7)	2.024(3)	1.914(3)	2.075(2)
M(1)–P(1)	2.256(1)	2.342(1)	2.338(1)	2.3370(7)	2.245(1)	2.3231(6)
M(1)–P(2)	2.234(9)[a]	2.349(1)	2.343(2)	2.3497(7)	2.242(1)	2.3555(6)
M(1)–P(3)	2.256(1)	2.329(1)	2.350(2)	2.3307(7)	2.235(1)	2.3247(6)
M(1)–P(4)	2.234(9)	2.348(1)	2.354(2)	2.3611(7)	2.216(1)	2.3470(6)
N(1)–C(5)	1.183(8)	1.161(5)	1.162(8)	1.157(3)	1.163(4)	1.159(3)
N(1)–B(1)				1.562(4)	1.604(4)	1.593(3)
N(1)–H(1N)		0.88(3)	0.95(1)			
N(1)···X[c]	2.9	2.7	2.8			
H(1N)···X[c]		1.82(3)	2.1			
P(1)–M(1)–P(2)	88.14(3)	83.48(4)	83.17(5)	82.69(3)	83.17(4)	84.78(2)
P(3)–M(1)–P(4)	85.14(3)	82.00(4)	81.94(5)	82.11(3)	83.77(4)	80.30(2)
P(1)–M(1)–C(5)	97.68(3)	98.4(1)	95.5(2)	96.61(7)	88.03(9)	96.76(6)
P(2)–M(1)–C(5)	91.35(3)	95.4(1)	97.3(2)	97.37(7)	97.56(9)	95.33(6)
P(3)–M(1)–C(5)	97.68(3)	87.1(1)	86.4(2)	86.94(7)	92.33(9)	89.66(6)
P(4)–M(1)–C(5)	91.35(3)	93.9(1)	94.1(2)	90.05(7)	110.49(9)	92.84(6)
H(1M)–M(1)–C(5)	180	173(2)	172(2)	175(1)		177.0(8)
N(1)–C(5)–M(1)	180	178.7(4)	178.3(6)	175.1(2)	177.4(3)	179.3(2)
C(5)–N(1)–B(1)				172.5(3)	178.4(3)	175.8(2)
H(1N)–N(1)–C(5)		174(6)	157(5)			

[a] From reference 2; the Fe(1)–P(2) distance was incorrectly reported; C(3) = C(5) of the present work. [b] From reference 7; C(53) = C(5) of the present work. [c] X = O(3) for complex **2Ru2** and F(3) for **2*Os2** in N(1)H–H(1N)···X hydrogen bond.

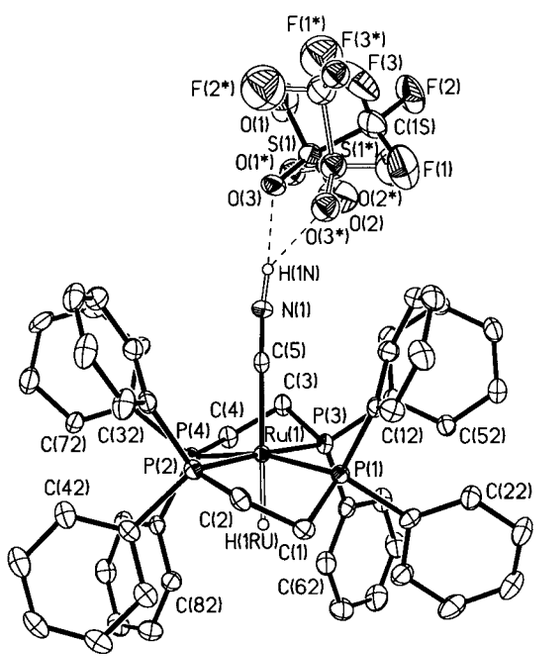

Fig. 1 Molecular structure of complex **2Ru2**.

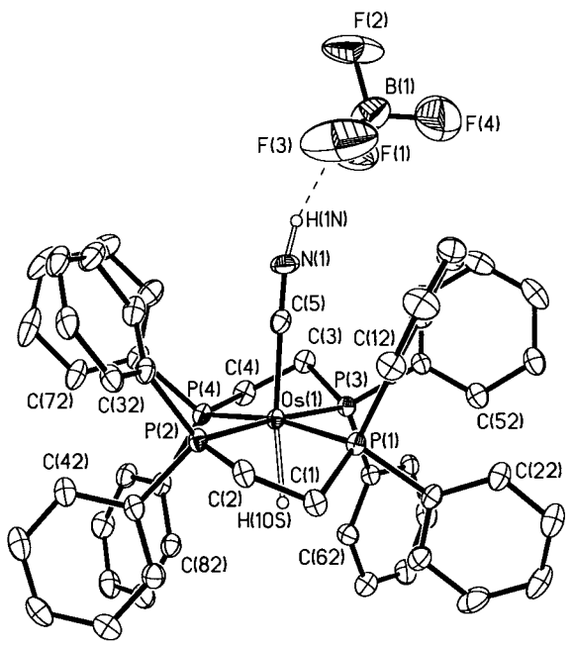

Fig. 2 Molecular structure of complex **2*Os2**.

2Ru2 to **5Ru2** and **6Ru2** (see Table 5 and below), the Ru–P, Ru–H and C–N distances are found to be very similar. The Ru–C(5) distance in **2Ru2** is, however, slightly shorter.

In the structure of **2Ru2** the triflate anion is disordered over two sites. The hydrogen atom of the hydrogen isocyanide ligand, however, is located in an electron density map, with an N–H distance of 0.88(3) Å. The H(1N)···O(3) distance in the CNH···triflate hydrogen bond is 1.82(3) Å. The N(1)···O(3) distance of 2.7 Å matches that of the hydrogen bond in $[RuCp(PPh_3)_2(CNH\cdots OTf)]$.[28]

In complexes **2*Fe5** and **2*Os2** the hydrogen of the hydrogen isocyanide ligand is hydrogen bonded to a neighbouring BF_4^- anion in each case. The N···F distances of 2.9 and 2.8 Å, respectively are less than the sum of the van der Waals radii of 3.1 Å (1.6 Å for N and 1.5 Å for F).[29]

For complexes **2Fe2**, **2Ru3** and **2Os3** the ν(MH) and ν(CN) modes in the IR spectra are detectable but usually of weak intensity and appear in the regions 2000–1800 and 2070–2050 cm^{-1}, respectively. These modes are likely to be coupled to each other. A ν(MH) mode was not detected for **2Os2** and **2Ru2**. For **2Ru2** the only peak in the 1800–3000 region is a broad, weak peak at 2500 cm^{-1}. A similar peak is observed in the IR spectrum of the compound methylaminoacetonitrile hydrochloride (CH_3NHCH_2CN·HCl).[30] The IR spectrum of *trans*-[RuH(CND)(dppe)$_2$]OTf **2Ru2-d** shows a medium intensity band, slightly broadened, at 2277 cm^{-1} with increased intensity as compared to **2Ru2**. The best explanation for these observations is that the vibrational modes of the O···HNCRuH unit are strongly coupled. Dega-Szafran and Szafran have investigated the effects of hydrogen bonding in some pyridine trifluoroacetates by infrared studies.[31,32] They noted a similar broad peak at 2500 cm^{-1} arising from all of the components of the complex absorption of ν(OH) and ν(NH) bands. Filarowski and Koll have noted a shifting to lower wavenumber and increase in intensity upon deuteriation of N···HO hydrogen bonds.[33]

The coupling of vibrations in all of the complexes complicates the interpretation of ν(CN) frequencies in terms of metal–carbon back donation. As noted by Almeida *et al.*[7] these modes are in the correct region for M–CNR and not for M–NCR compounds.

The NMR spectra of complex **2M*j*** indicate that a *trans*-octahedral geometry is maintained in solution. The hydride resonances of the complexes appear as quintets and the phosphorus resonances of the ^{31}P-{^{1}H} NMR spectra are singlets. For comparable compounds **2M*j*** there is a shift ($\Delta\delta$) of the hydride resonance of 2.0 ppm downfield and about 1 ppm upfield on going from Fe to Ru and from Ru to Os, respectively. When the diphosphine is changed from dppe to dppp the hydride shifts 1.7 ± 0.1 ppm downfield. This shift is similar to that observed for the *trans*-[MH(CN)L_2] complexes. For the **2M2** complexes the NH resonance was observed in the proton NMR spectra as a triplet in the region between δ 10.5 and 9.5 with $^{1}J(^{1}H,^{14}N) = 80$, 73 or 81 Hz for **2Fe2**, **2Ru2** or **2Os2**, respectively. This is strong evidence for the presence of coordinated hydrogen isocyanide as opposed to hydrogen cyanide.

The use of isotopically labelled cyanide in the preparation of compounds **2M*j*** also serves to prove that the ligand is coordinated as MCNH and not MNCH. Representative data for the complexes **2M3-n** (with MC^{15}NH) and **2M3-c** (with M^{13}CNH) are listed in Table 4. The signal of the CNH proton was not observed at room temperature in the ^{1}H NMR spectrum of **2Ru3** or **2Os3** probably due to a rapid proton exchange process. However at −90 °C a broad N^{1}H signal was detected at δ 10.7 or 10.4, respectively. For the compounds **2M3-n** that are prepared *in situ* in CD_2Cl_2 by 1:1 reaction of **1M3-n** with HOTf these signals are doublets with $^{1}J(H,^{15}N) = 115.7$ or 116.9 Hz, respectively. In the NMR spectra of the compounds **2M3-c** the observation of ^{2}J(P,C) coupling constants of 10 Hz for **2Ru3-c** and 7 Hz for **2Os3-c** also support the proposal of a M–CNH coordination mode.

Synthesis and properties of *trans*-[MH(CNBF$_3$)L_2]

Complexes containing the $CNBF_3^-$ ligand are usually obtained when **1M*j*** in CD_2Cl_2 are treated with HBF_4·Et_2O. For example, three species are produced when one equivalent of 85% HBF_4· Et_2O is added to complex **1Ru2** in CD_2Cl_2 (eqn. (1)). The

$$HBF_4 + \underset{}{\mathbf{1Ru2}} \longrightarrow \underset{\mathbf{5Ru2}}{[RuH(CNBF_3)L_2]} + [Ru(H_2)(CNBF_3)L_2]^+ + \text{unidentified} \quad (1)$$
$$\mathbf{7?Ru2}$$

^{1}H NMR spectrum has a quintet at δ −9.6 (^{2}J(HP) = 19.4 Hz) for **5Ru2** and a broad singlet at δ −6.1 attributed to **7?Ru2** that has an unidentified counter ion (the question mark indicates that it may be BF_4^-, or more likely FHF^-). The ^{31}P-{^{1}H} NMR spectrum revealed three singlets at δ 67.3 (**5Ru2**), 53.1 (**7?Ru2**) and 49.8 (unidentified). The species **7?Ru2** has similar chemical shifts to **7Ru2-d** (see below). The unidentified species might be *trans*-[Ru(BF_4)(CN)(dppe)$_2$] since the chemical shift is similar to that of *trans*-[Ru(OTf)(CN)(dppe)$_2$] (δ 52.1).[5]

Complex **5Ru2** was independently synthesized by treating one equivalent of BF_3·Et_2O with **1Ru2** (Scheme 2, step i) and characterized by X-ray diffraction (Fig. 3), microanalysis (Table 2) and spectroscopy (Tables 2 and 3). The hydride in the octahedral complex **5Ru2** is located from an electron density map with an Ru–H bond distance of 1.67(3) Å. The dimensions of the $HRuP_4CN$ core are very similar to those of **2Ru2** (Table 5). Weigand *et al.*[14] have studied the addition of HBF_4·Et_2O to [RuCp(CN)(PPh_3)$_2$] to produce [RuCp($CNBF_3$)(PPh_3)$_2$] as shown by an X-ray diffraction study. The bond lengths and angles of the $RuCNBF_3$ fragment are very similar to those determined for **5Ru2**.

When one equivalent of [$HPPh_3$]BF_4 is added to **1Os2**, *trans*-[OsH(CNH)(dppe)$_2$]BF_4 **2*Os2** is formed (Scheme 2, step ii).

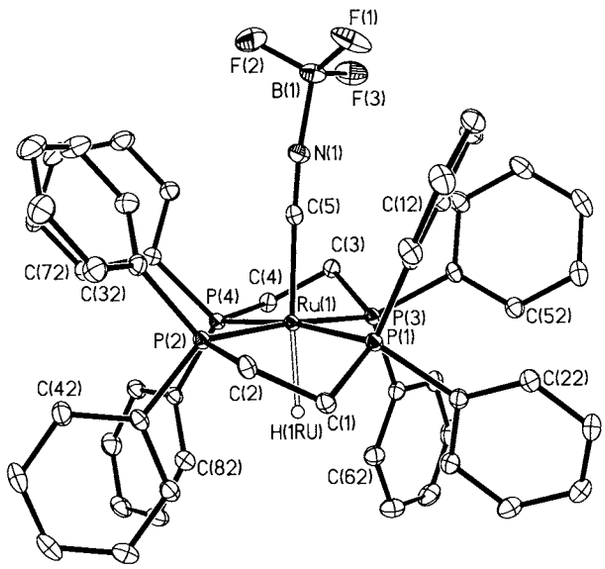

Fig. 3 Molecular structure of complex **5Ru2**.

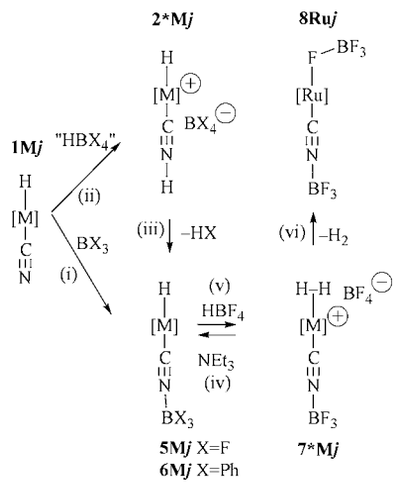

Scheme 2

In solution, over a period of months, it rearranges to *trans*-[OsH($CNBF_3$)(dppe)$_2$] **5Os2** (step iii) with the spectroscopic properties shown in Table 3.

Compounds **5Ru3** and **5Os3** were prepared by deprotonating the respective dihydrogen complexes **7*M3** (see below) with NEt_3 (Scheme 2, step iv). The ^{1}H and ^{31}P NMR data are consistent with distorted octahedral structures (Table 3). The presence of the BF_3 ligand was confirmed by ^{19}F NMR spectroscopy (Table 3).

The reaction of complex **1Ru3** with HBF_4·Et_2O in CH_2Cl_2 is complicated because of the formation of species containing the $CNBF_3^-$ ligand. Thus the ^{31}P-{^{1}H} NMR spectrum of a 48 mM solution of **1Ru3** in the presence of an equimolar amount of HBF_4·Et_2O shows after 30 min the presence of **5Ru3** (11%), **2*Ru3** (42%), [Ru(H_2)(CN)(dppp)$_2$]BF_4 (**3*Ru3**, 34%), **7*Ru3** (11%) and a small amount (2%) of the complex *trans*-[Ru(FBF_3)($CNBF_3$)(dppp)$_2$] **8Ru3**. On standing an increase in the $CNBF_3$-containing species is observed and after 19 hours the composition is: **5Ru3** (28%), **2*Ru3** (24%), **3*Ru3** (25%), **7*Ru3** (18%) and **8Ru3** (5%). The addition of Et_2O to the reaction mixture favours the transformation of **2*Ru3** into **5Ru3**. The results of experiments that were carried out with the ^{13}CN enriched compound **1Ru3-c** support these assignments. Thus the ^{13}C-{^{1}H} NMR spectrum in the CN region shows the $CNBF_3^-$ resonances of **5Ru3-c**, **7*Ru3-c** and **8Ru3-c** and the CNH resonance of **2*Ru3-c**. As expected all the ^{31}P-{^{1}H} signals are doublets with the J(P,C) ranging between 9.5 and 14.3 Hz, while the hydride signals of **2*Ru3-c** and **5Ru3-c** are

quintets of doublets, owing to the coupling of the hydride with the ^{31}P nuclei and the ^{13}C nucleus of the ^{13}CNH ligand or of the $^{13}CNBF_3^-$ group.

NMR measurements show that the protonation of complex **1Os3** with $HBF_4{\cdot}Et_2O$ in CH_2Cl_2 leads to the initial formation of **2*Os3** and **5Os3** which are, in turn, protonated to $[Os(H_2)(CNH)(dppp)_2][BF_4]_2$ **4*Os3**[5] and **7*Os3**. This reaction is slower than that with ruthenium complexes and in the long run the $CNBF_3^-$ derivatives become predominant. The investigation of this reaction is complicated because the dihydrogen complexes exhibit very similar ^1H and ^{31}P NMR signals.

Comparing the proton NMR data of complexes **5Ru2**, **5Os2**, **5Ru3** and **5Os3**, we note that the hydride resonance shifts 1.1 ± 0.1 ppm upfield when Ru is changed to Os. A similar trend is observed for the **1M*j*** and **2M*j*** series. When the diphosphine ligand is changed from dppe to dppp the hydride resonance is shifted by 1.8 ± 0.1 ppm downfield, comparable to the other series above. When the hydride resonances of **5M*j*** are compared to those of **1M*j*** a downfield shift is noted as the CN^- ligand is substituted by $CNBF_3^-$.

From IR spectroscopic studies of complexes **5M*j***, the *ν*(MH) mode is observed in the region 1970–1870 cm^{-1} and the *ν*(CN) mode in the region 2140–2110 cm^{-1}. Both the *ν*(MH) and *ν*(CN) modes of the $CNBF_3^-$ complexes are observed at a higher frequency than those of **1M*j***.

Synthesis and properties of *trans*-[MH(CNBPh$_3$)L$_2$]

The compound *trans*-$[RuH(CNBPh_3)(dppe)_2]$ **6Ru2** was first obtained as a side product when crude **1Ru2**, that was contaminated with $KBPh_4$, was protonated with HOTf (Scheme 2, steps (ii) and (iii)). It was independently prepared by the addition of one equivalent of BPh_3 to **1Ru2** (Scheme 2, step (i)). An X-ray diffraction study, microanalysis and spectroscopy confirm its identity. In the IR spectrum the *ν*(CN) mode is observed at 2124 cm^{-1} but the MH mode is not detected. The ^1H and ^{31}P data (Table 3) are consistent with a *trans*-octahedral structure.

The structure and dimensions of the $HRuP_4CNB$ core fragment of complex **6Ru2** (Fig. 4) are very similar to those of **5Ru2**. The B–N bond length of **6Ru2** (1.593(3) Å) is slightly longer than the one determined for **5Ru2** (1.562(4) Å). This is probably due to steric interactions between the Ph groups of the $CNBPh_3^-$ ligand and the Ph groups of the dppe ligands in complex **6Ru2**. The smaller BF_3 group experiences less steric repulsion. On the other hand this could be explained by the fact that BF_3 is a stronger Lewis acid than BPh_3 and therefore makes a shorter bond. The C–N bond lengths of **5Ru2** and **6Ru2** are the same, although the *ν*(CN) stretching frequency of the former is higher.

The dimensions of the $HFeP_4C$ core of the related complex *trans*-$[FeH(CNBPh_3)(dppe)_2]$ **6Fe2**[7] are uniformly smaller than those found in **6Ru2** as expected (Table 5). The *ν*(CN) mode of **6Fe2** (2090 cm^{-1}) is lower than that of **6Ru2** while the C–N bond lengths from X-ray diffraction are essentially equivalent. This can be explained by Fe being the stronger π-back bonder. The angles M–C–N are comparable. One might have expected that repulsions between the phenyl groups of the BPh_3 and the dppe ligands in the smaller **6Fe2** compound would be greater than those in **6Ru2** but this is not reflected in the N–B distances that are the same in the two structures. Instead the C(5)–M–P angles provide evidence that the dppe ligands in the iron complex are pushed away from the $CNBPh_3^-$ ligand. The average C(5)–M–P angles are 97 (Fe) and 94° (Ru) with one C(5)–Fe–P as large as 110.5(1)°. However, as in the case of complexes **2M**, the M–P bond distances do not vary greatly.

In a control experiment $[HPPh_3]BF_4$ was added to $KBPh_4$ in toluene. No reaction occurred as indicated by the $^{31}P\text{-}\{^1H\}$ NMR spectrum. Thus the hydrogen isocyanide ligand plays an important role in cleavage of the B–C bond. Amrhein *et al.* have also observed a similar reaction where BPh_3 is abstracted from $NaBPh_4$ under acidic conditions to form the complex $[Fe(TIM)(CNBPh_3)_2]$ (TIM = 2,3,9,10-tetramethyl-1,4,8,11-tetraazacyclotetradeca-1,3,8,10-tetraene).[15] Certainly the well known affinity of the CN ligand for BPh_3[34] helps to drive the reaction.

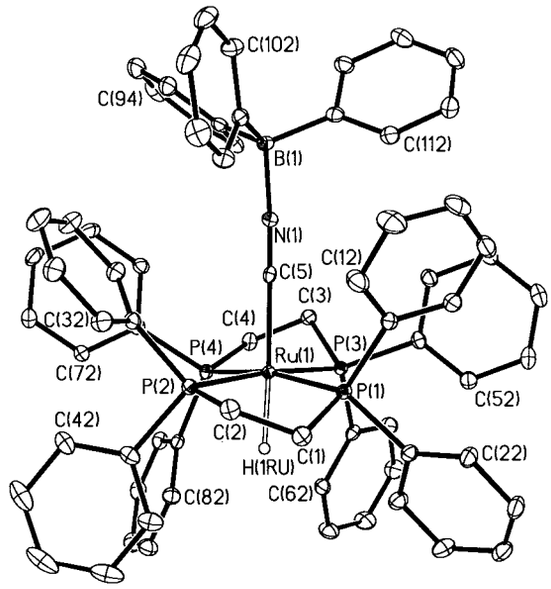

Fig. 4 Molecular structure of complex **6Ru2**.

Preparation and properties of *trans*-[M(H$_2$)(CNBF$_3$)L$_2$]$^+$

When complex **1Ru3** is treated with $HBF_4{\cdot}Et_2O$ in benzene in a 1 : 2 molar ratio, white crystals of the complex *trans*-$[Ru(\eta^2\text{-}H_2)(CNBF_3)(dppp)_2]BF_4$ **7*Ru3** are immediately formed. The infrared spectrum shows a strong peak at 2174 cm^{-1} for the *ν*(CN) of the $CNBF_3^-$ ligand. The high-field ^1H NMR spectrum exhibits a very broad peak at δ −4.3 for the dihydrogen ligand with a T_1 minimum of 5 ms at −50 °C and 200 MHz. The analogous η^2-HD complex **7Ru3-d** (obtained by addition of excess of DOTf to **5Ru3**) produces a 1 : 1 : 1 triplet at δ −4.3 with $^1J(H,D)$ 32.7 Hz. These data suggest the presence of a "fast-spinning" dihydrogen ligand with an H–H distance of 0.87 Å.[35] The $^{31}P\text{-}\{^1H\}$ NMR spectrum exhibits a broad singlet at δ 9.1, which resolves into the usual A_2X_2 system at δ 2.7 and 15.9 ($J(P,P')$ = 28.7 Hz) at −90 °C.

The presence of the $CNBF_3^-$ ligand and BF_4^- ion in complex **7*Ru3** is confirmed by analysing the $^{19}F\text{-}\{^1H\}$ NMR spectrum in CD_2Cl_2 where two signals that integrate 4 : 3 are present at δ −152.0 and at −146.8. These signals, due to the fluorine bonded to ^{11}B (isotopic abundance 81%), are accompanied by signals of minor intensity due to the fluorine bonded to ^{10}B (isotopic abundance 19%) shifted by 0.05 ppm.

The complex **7*Ru3** reacts with NEt_3 to give the hydride complex **5Ru3** as noted above. In addition, in CH_2Cl_2 solution with argon bubbling it loses hydrogen to give white needles of the new compound $[Ru(FBF_3)(CNBF_3)(dppp)_2]$ **8Ru3** (Scheme 2). The IR spectrum of a Nujol mull shows the strong *ν*(CN) absorption of the $CNBF_3^-$ group at 2126 cm^{-1} while the ^{19}F NMR spectrum in CD_2Cl_2 solution exhibits two signals at δ −151.3 and −147.4 which can be attributed to the fluorine atoms of the coordinated BF_4^- and BF_3 groups respectively. The ^{31}P NMR spectrum in CD_2Cl_2 shows at room temperature a single signal at δ 2.8 which at −90 °C splits in two triplets at δ −1.4 and 0.7 with a $J(P,P)$ = 30.0 Hz. For **8Ru3-c** there are two ^{19}F resonances at δ −152.0 (s) and −146.8 (d, $J(F,^{13}C)$ = 5.6 Hz).

The complexes **7*Os3** and **7Os3-d** are prepared in a similar fashion to **7*Ru3** and **7Ru3-d**. The evidence for the dihydrogen

ligand is a broad resonance in the ^{1}H NMR spectrum at δ −4.7 with a T_1(min) of 6 ms at −50 °C, 200 MHz for **7*Os3** and a 1:1:1 triplet at δ −4.7 with ^1J(H,D) 28.0 Hz for **7Os3-d**. These data suggest the presence of a "slow-spinning" dihydrogen ligand with an H–H distance of 0.95 Å.[35]

Excess of deuteriated triflic acid (DOTf) was added to an NMR tube containing either complex **5Ru2** or **6Ru2** in CD_2Cl_2 to investigate the properties of the η^2-HD complexes *trans*-[Ru(η^2-HD)($CNBF_3$)(dppe)$_2$]OTf **7Ru2-d** and *trans*-[Ru(η^2-HD)($CNBPh_3$)(dppe)$_2$]OTf. For complex **7Ru2-d** a characteristic 1:1:1 triplet with ^1J(HD) = 32.6 Hz is observed in the hydride region of the ^{1}H NMR spectrum at δ −6.0. From the coupling constant, the H–H distance of the dihydrogen complex is calculated to be 0.88 Å.[36] A singlet at δ 52.0 is observed in the ^{31}P-{^{1}H} NMR spectrum. Similarly the HD complex containing the $CNBPh_3^-$ ligand also produces a 1:1:1 triplet with ^1J(HD) = 32.5 Hz at δ −6.0 and a singlet at δ 51.8 for the ^{31}P nuclei.

Electrochemical measurements

The electrochemical potentials for the reversible d^5/d^6 redox change at the metal of selected complexes as determined by cyclic voltammetry are listed in Table 6. The iron complex **1Fe2** is more reducing than its osmium analogue **1Os2**. This is consistent with the lower ν(CN) for **1Fe2** (Table 2). The same $E_{1/2}$ value for **1Fe2** has already been reported.[7] The dppp ligand makes **1Os3** more reducing than the dppe ligand in **1Os2** by 50 mV while the dtpe ligand makes **1Fe5** more reducing than the dppe ligand in **1Fe2** by 100 mV. Again, the corresponding ν(CN) values reflect this change. The fact that **1Ru3** is more reducing than **1Os3** is not consistent with the IR results where the osmium compound has the slightly lower ν(CN) value; this is not understood. In the presence of acid, **2Fe2** shows a reversible redox wave at 0.15 V. A kinetic analysis of the electrochemical behaviour of **2Fe2** in the absence of added acid provided a similar value.[7] The fact that *trans*-[FeH(CNMe)(dppe)$_2$]$^+$ has $E_{1/2}$ 0.38 V shows that the CNH ligand makes the iron more reducing than the CNMe ligand by 0.2 V.[37]

Conclusion

Cyanide and hydrogen isocyanide complexes have been prepared in high yield. The trends in ν(CN) of **1M*j*** are found to be Fe < Os ≤ Ru, dppp < depe < dppe < dppm, while there are no obvious trends for the series **2M*j*** due to coupling of vibrational modes. There are systematic changes in NMR chemical shifts upon changing in turn the metal, the diphosphine, and CN *vs.* CNH *vs.* $CNBF_3$. Use of $^{13}CN^-$ or $C^{15}N^-$ as ligand provides evidence for the MCNH coordination mode over MNCH. Structures of hydrogen isocyanide compounds with M = Fe, Ru or Os have now been determined. Those of Ru and Os are very similar while the iron complex has greater inter-ligand repulsions. The CNH ligand is a good hydrogen-bond donor so that NH · · · F or NH · · · O hydrogen bonds with the counter ion are formed in each case.

Compounds with $CNBF_3^-$ and $CNBPh_3^-$ ligands can be prepared by reaction of BX_3 with **1M*j*** or BX_4^- with **2M*j***. Reaction (2) with X = F or Ph seems particularly favourable

$$[M]CNH^+ + BX_4^- \longrightarrow [M]CNBX_3 + HX \qquad (2)$$

kinetically and thermodynamically. The reactions involve the elimination of HF or HPh that are very weak acids in CH_2Cl_2. The reaction is kinetically more favourable than that of $HPPh_3^+$ with BPh_4^-.

This suggests that the small CNH group can readily attack the BF or BC bonds whereas other larger acids of comparable acidity do not react. The large $CNBPh_3$ group appears to push away the dppe ligands in **5*Fe2** more than in **5Ru2** and this results in large C–M–P angles while normal M–P distances are maintained. When the ligands are changed from CN^- to $CNBPh_3^-$ or $CNBF_3^-$, the ν(CN) stretching frequencies increase (CN^- < $CNBPh_3^-$ < $CNBF_3^-$) as expected on the basis of the Lewis acid strength. The new dihydrogen complexes *trans*-[M(H_2)($CNBF_3$)L_2]$^+$ have been characterized spectroscopically. The dihydrogen ligand in the ruthenium complex **7*Ru3** is readily substituted by BF_4^-.

Table 6 Electrochemical data (V *vs.* Fe(C_5H_5)$_2^{+/0}$) for selected complexes in THF[a]

Compound	$E_{1/2}$($M^{III/II}$)/V
1Fe2 [FeH(CN)(dppe)$_2$]	−0.22
1Os2 [OsH(CN)(dppe)$_2$]	0.23
1Ru3 [RuH(CN)(dppp)$_2$]	0.13
1Os3 [OsH(CN)(dppp)$_2$]	0.18
1Fe5 [FeH(CN)(dtpe)$_2$]	−0.32
2Fe2 [FeH(CNH)(dppe)$_2$]OTf	0.15[b]

[a] 0.2 M NBu_4PF_6 as electrolyte, reversible reductions. [b] [$HPPh_3$]OTf added (0.01 M) to suppress H^+ dissociation.

Experimental

General procedures

All manipulations were carried out under Ar in a Vacuum Atmosphere glovebox or by use of Schlenk-line techniques, unless otherwise noted. Solvents were purified by standard methods. Reagent-grade chemicals and NMR solvents were used as purchased from Aldrich. The ligands dppm and dppp as well as the compound $(NH_4)_2OsCl_6$ were purchased from Aldrich. Digital Specialty Chemicals Ltd. donated the phosphine ligand dppe while depe was purchased from Organometallics Inc. Complexes *trans*-[RuH(η^2-H_2)(dppe)$_2$]BPh_4 and *trans*-[$RuCl_2$(depe)$_2$] were prepared according to literature methods.[38] The dtpe was prepared by the method of Chatt *et al.*[39] [$HPPh_3$]OTf and [$HPPh_3$]BF_4 were prepared in a similar fashion to [HP(C_6H_4Me-*p*)$_3$]BF_4, by treating PPh_3 with HOTf or HBF_4·Et_2O, respectively.[40] Slow evaporation of the solvent into the argon atmosphere of a glovebox provided a means of crystal growth for some of the compounds. The cyclic voltammetry apparatus has been described.[41]

For complexes containing dppe or depe, NMR spectra were obtained on a Varian Gemini 300 spectrometer, operating at 300 MHz for ^{1}H and 120.5 MHz for ^{31}P-{^{1}H} (referenced to 85% H_3PO_4). All ^{31}P NMR spectra were proton decoupled. Chemical shifts refer to room temperature conditions unless otherwise stated. ^{1}H NMR T_1 measurements were made using the inversion recovery method.[42] Infrared spectra were recorded on a Nicolet 5DX FTIR spectrometer on samples as Nujol mulls on NaCl plates. Microanalyses were performed by Guelph Chemical Laboratories Ltd., Guelph, ON.

For complexes containing dppm or dppp, NMR spectra were obtained with a Bruker AC 200 spectrometer. All ^{31}P-{^{1}H} NMR spectra were referenced to 85% H_3PO_4. Infrared spectra were recorded on a Nicolet Magna 550 FT-IR spectrophotometer. Microanalyses were performed by the Microanalytical Laboratory of the Dipartimento di Scienze e Tecnologie Chimiche, Università di Udine.

Preparations

***trans*-[FeH(Cl)(dtpe)$_2$].** dtpe (0.12 g, 0.56 mmol) was dissolved in 30 mL THF and $FeCl_2$ (35 mg, 0.28 mmol) added. To the resulting tan-coloured solution, $NaBH_4$ (10 mg, 0.28 mmol) was added along with 5 mL ethanol. The solution was stirred for one hour. This dark red solution was filtered through Celite, the volume reduced to about 2 mL and 5 mL hexanes were added. A red precipitate (54% yield) was filtered off and

washed with a small amount of diethyl ether. $\delta(^1H, C_6D_6)$ −29.1 (q, 48 Hz). FAB MS: *m*/*z* 1000.8 (M^+).

***trans*-[RuH(Cl)(depe)$_2$].** Reported here is a more convenient route for synthesizing *trans*-[RuH(Cl)(depe)$_2$] than previously published.[26] In a nitrogen glovebox, a round bottom flask was charged with *cis*-[$RuCl_2$(depe)$_2$] (0.936 g, 1.702 mmol) and 20 mL of MeOH. The bright yellow solution was stirred and $NaBH_4$ (0.060 g, 1.586 mmol) slowly added, causing effervescence. The resulting dark yellow solution was left to stir for approximately 15 h. Filtering removed the white precipitate (NaCl and borates) that formed. The solvent was removed *in vacuo*, leaving a dark yellow residue.

***trans*-[RuH(CN)(dppm)$_2$] 1Ru1.** *trans*-[RuH(Cl)(dppm)$_2$][26] (2.43 g, 2.68 mmol) and NaCN (0.24 g, 4.90 mmol) were dissolved in a mixture of 30 mL of CH_2Cl_2, 20 mL of MeOH and 5 mL of water. After stirring at room temperature for 2 h, the organic solvents were evaporated under vacuum, and the water layer was decanted. The crude white-cream product was dried under vacuum and recrystallized from C_6H_6–hexane.

***trans*-[OsH(CN)(dppm)$_2$] 1Os1.** *trans*-[OsH(Cl)(dppm)$_2$][26] (0.25 g, 0.25 mmol) and NaCN (20 mg, 0.41 mmol) were dissolved in a mixture of 10 mL of CH_2Cl_2, 10 mL of MeOH and 3 mL of water. After stirring at room temperature for 5 h, the organic solvents were evaporated under vacuum, and the water layer was decanted. The crude white product was dried under vacuum and recrystallized from C_6H_6–hexane.

***trans*-[FeH(CN)(dppe)$_2$] 1Fe2.** A route to this complex was recently published.[7] We report a different method requiring less time and using different reagents. A solution of KCN (150 mg, 2.3 mmol) in MeOH (5 mL) was added to a purple solution of *trans*-[FeH(Cl)(dppe)$_2$][43] (1.0 g, 1.1 mmol) in THF (70 mL) and the mixture stirred for 1 h. The solvent was removed from the orange solution and the product extracted into toluene. Removal of the toluene left an orange powder.

***trans*-[FeH(CN)(dtpe)$_2$] 1Fe5.** The preparation followed that of **1Fe2** with the replacement of KCN with NaCN. FAB MS: *m*/*z* 990.0 (M^+).

***trans*-[RuH(CN)(dppe)$_2$] 1Ru2.** Upon entering the argon glovebox, the solid *trans*-[RuH(η^2-H_2)(dppe)$_2$]BPh_4 that is off white when stored under H_2 changed to a deep orange. This sample (45 mg, 0.37 mmol) was suspended in 20 mL of methanol and KCN (40 mg, 0.61 mmol) added with stirring. The suspension turned from orange to white after 1 hour. The reaction mixture was stirred overnight. The white *trans*-[RuH(CN)(dppe)$_2$] was filtered off, washed with 5 mL of MeOH and dried *in vacuo*. Purification of the product involved dissolving it in toluene and filtering off the salt. Evaporation of the solvent produced a white solid.

***trans*-[OsH(CN)(dppe)$_2$] 1Os2.** *trans*-[OsH(Br)(dppe)$_2$][36] (0.270 g, 0.253 mmol) was dissolved in 4 mL of CH_2Cl_2 forming a yellow solution. When 2 mL of methanol were added the solution became slightly brown. Addition of KCN (0.033 g, 0.506 mmol) changed it back to yellow. After stirring continuously for 16 h, a white precipitate formed in a colourless solution. The solvent was removed under vacuum and 2 mL of an 80 : 20 mixture of methanol–water were added to the solid and the reaction mixture was stirred for 5 min. The solid was filtered off, washed twice with the methanol–water mixture, once with methanol, followed by diethyl ether before drying under a vacuum.

***trans*-[RuH(CN)(dppp)$_2$] 1Ru3.** *trans*-[RuH(Cl)(dppp)$_2$][44] (0.35 g, 0.36 mmol) and KCN (30 mg, 0.46 mmol) were suspended in a mixture of 10 mL of CH_2Cl_2, 10 mL of MeOH, and 10 mL of water. After stirring at room temperature for 2 h, the organic solvents were evaporated in vacuum, and the water layer was decanted. The crude white product was dried under vacuum and recrystallized from C_6H_6–hexanes. The microcrystalline product contains 1 C_6H_6 molecule per mole of complex (by ^1H NMR).

***trans*-[OsH(CN)(dppp)$_2$] 1Os3.** *trans*-[OsH(Cl)(dppp)$_2$][45] (0.40 g, 0.38 mmol) and KCN (30 mg, 0.46 mmol) were treated as described for the ruthenium analogue. The crude white product was dried *in vacuo* and recrystallized from a C_6H_6–hexane mixture. The microcrystalline product contains 2 C_6H_6 molecules per mole of complex as evidenced by ^1H NMR.

***trans*-[FeH(CN)(depe)$_2$] 1Fe4.** A solution of KCN (123 mg, 1.89 mmol) in MeOH (5 mL) was added to a solution of *trans*-[FeH(Cl)(depe)$_2$][46] (954 mg, 1.89 mmol) in MeOH (15 mL) and the mixture stirred for 1 h to give a yellow suspension. The solvent was removed *in vacuo*, the product extracted into toluene, and the KCl removed by filtration. The product was isolated as a yellow powder.

***trans*-[RuH(CN)(depe)$_2$] 1Ru4.** *trans*-[RuH(Cl)(depe)$_2$] (0.800 g, 1.454 mmol) was dissolved in 10 mL of MeOH producing a clear dark yellow solution. KCN (0.111 g 1.705 mmol) was added and the solution stirred for approximately 15 h. The solvent was removed *in vacuo* and the light yellow residue dissolved in 5 mL of toluene and filtered. The solvent was removed again and large light yellow crystals were obtained by slow evaporation of a saturated solution of complex **1Ru4** in C_6H_6.

***trans*-[OsH(CN)(depe)$_2$] 1Os4.** *trans*-[OsH(Cl)(depe)$_2$][26] (0.100 g, 0.156 mmol) was dissolved in 5 mL of methanol. Excess of KCN (0.021 mg, 0.312 mmol) was added and stirred for 16 h, yielding a colourless solution. The solvent was removed under vacuum and then 5 mL toluene were added to the white residue and stirred for 20 min. The reaction mixture was filtered and the toluene solution concentrated. Large colourless needles were obtained by slow evaporation of the concentrated solution.

***trans*-[RuH(CNH)(dppm)$_2$]OTf 2Ru1.** *trans*-[RuH(CN)(dppm)$_2$] (0.20 g, 0.22 mmol) was suspended in 5 mL of toluene. Upon addition of CF_3SO_3H (20 μl, 0.23 mmol) the solution was stirred at room temperature for 10 minutes. Then, 20 mL of Et_2O were added obtaining a white precipitate, which was filtered off, washed with ether, dried under vacuum and recrystallized from CH_2Cl_2–Et_2O.

***trans*-[OsH(CNH)(dppm)$_2$]OTf 2Os1.** *trans*-[OsH(CN)(dppm)$_2$] (0.11 g, 0.11 mmol) was suspended in 10 mL of Et_2O. Upon addition of CF_3SO_3H (10 μl, 0.11 mmol) the solution was stirred at room temperature for 10 minutes. Then, a pale green precipitate was formed, which was filtered off, washed with ether, dried in vacuum and recrystallized from CH_2Cl_2–Et_2O.

***trans*-[FeH(CNH)(dppe)$_2$]OTf 2Fe2.** Some of us have previously published the synthesis of the BF_4 analogue, *trans*-[FeH(CNH)(dppe)$_2$]BF_4.[2] Another group has recently published a different route to the BF_4 analogue.[7] We report here complexes containing the OTf anion.

Method 1. Protonation of **1Fe2** (100 mg, 0.11 mmol) in CD_2Cl_2 (8 mL) with 1 equivalent of HOTf (17 mg, 0.11 mmol) produced **2Fe2**.

Method 2. Addition of [Ph_3PH]OTf (15 mg, 0.036 mmol) to a solution of **1Fe2** (31 mg, 0.032 mmol) in CD_2Cl_2 (1 mL) produced **2Fe2**. Evaporation of the solvent yielded a yellow powder that was washed with Et_2O.

***trans*-[RuH(CNH)(dppe)$_2$]OTf 2Ru2.** *Method 1.* Triflic acid (29 mg, 0.19 mmol) was added to 3 mL of benzene and stirred. In a separate flask, *trans*-[RuH(CN)(dppe)$_2$] (178 mg, 0.19 mmol) was added to 5 mL of benzene and the white suspension stirred. The white suspension was added to the triflic acid solution and the clear colourless reaction mixture stirred for 1 hour, producing a white suspension. The solvent was decanted and the white product washed with 5 mL of benzene and then dried *in vacuo*. Suitable crystals for structure determination were grown by slow evaporation of a concentrated solution of the product in CH_2Cl_2, producing clear colourless crystals in 97% yield.

Method 2. Triphenylphosphonium triflate (44.6 mg, 0.11 mmol) was added to a solution of *trans*-[RuH(CN)(dppe)$_2$] (100 mg, 0.11 mmol) in 5 mL of benzene and the white suspension stirred. After half an hour the solvent was decanted and the white precipitate washed with ether and dried *in vacuo*.

Method 3. H_2 gas was bubbled into an NMR tube containing a solution of *trans*-[Ru(OTf)(CNH)(dppe)$_2$]OTf[5] (13.9 mg, 0.011 mmol) in 0.8 mL of CD_2Cl_2. PPh_3 (1.8 mg, 6.9×10^{-3} mmol) was added to produce a solution containing **2Ru2**.

Method 4. An NMR tube containing *trans*-[Ru(OTf)(CN)(dppe)$_2$][5] (0.02 g, 0.02 mmol) was dissolved in approximately 0.08 mL of CD_2Cl_2. H_2 gas was bubbled through the solution and **2Ru2** was observed to form.

***trans*-[RuH(CND)(dppe)$_2$]OTf 2Ru2-d.** A method similar to Method 1 for complex **2Ru2** was followed except DOTf was used instead of HOTf.

***trans*-[OsH(CNH)(dppe)$_2$]Y 2Os2 (Y = OTf), 2*Os2 (Y = BF_4).** *trans*-[OsH(CN)(dppe)$_2$] (0.060 g, 0.059 mmol) was dissolved in 6 mL of toluene. [$HPPh_3$]OTf (0.025 g, 0.059 mmol) was then added and the solution stirred. After 30 min a white precipitate was formed. After removal of the solvent by decanting, the solid was washed twice with 4 mL of toluene and then dried *in vacuo*. **2*Os2** was prepared similarly except [$HPPh_3$]BF_4 was used instead of HOTf. Colourless crystals of **2*Os2** suitable for structure determination were formed by slow diffusion of Et_2O into a concentrated solution of the complex in CH_2Cl_2.

***trans*-[RuH(CNH)(dppp)$_2$]OTf 2Ru3.** *trans*-[RuH(CN)(dppp)$_2$] (0.20 g, 0.21 mmol) was suspended in 10 mL of Et_2O. Upon addition of HOTf (20 μl, 0.23 mmol), the solution was stirred at room temperature for 10 minutes. A pale yellow precipitate formed which was filtered off, washed with ether, dried under a vacuum and then recrystallized from a CH_2Cl_2–hexanes mixture.

***trans*-[OsH(CNH)(dppp)$_2$]OTf 2Os3.** *trans*-[OsH(CN)(dppp)$_2$] (0.20 g, 0.19 mmol) was suspended in 10 mL of Et_2O. Upon addition of HOTf (20 μl, 0.23 mmol), the solution was stirred at room temperature for 10 minutes. A pale pink precipitate formed which was filtered off, washed with ether, dried under a vacuum and then recrystallized from a CH_2Cl_2–hexanes mixture. The microcrystalline product contains $\frac{1}{2}$ C_6H_{14} molecule per mole of complex (by ^{1}H NMR).

***trans*-[RuH(CNBF_3)(dppe)$_2$] 5Ru2.** *Method 1.* $HBF_4 \cdot Et_2O$ (12 mg, 0.07 mmol) was added to a solution of *trans*-[RuH(CN)(dppe)$_2$] (0.05 g, 0.05 mmol) in 5 mL of benzene. After stirring for 30 min, the white product was filtered off, washed with 5 mL of benzene and dried *in vacuo*. The NMR spectra (^{1}H and ^{31}P-{^{1}H}) of the crude product revealed a mixture of complex **5Ru2** and two other unidentified complexes (^{1}H, δ −6.1; ^{31}P-{^{1}H}, δ 53.1; ^{31}P{^{1}H}, δ 49.8). Colourless crystals suitable for structure determination were obtained by slow evaporation of a concentrated solution of the product in CH_2Cl_2.

Method 2. [$HPPh_3$]BF_4 (0.05 g, 0.14 mmol) was added to a solution of *trans*-[RuH(CN)(dppe)$_2$] (0.13 g, 0.14 mmol) in 5 mL of benzene. The white suspension was stirred for 30 min, then filtered, washed with 5 mL of benzene and dried *in vacuo*.

Method 3. Addition of $BF_3 \cdot Et_2O$ (0.03 g, 0.21 mmol) to a solution of *trans*-[RuH(CN)(dppe)$_2$] (0.10 g, 0.11 mmol) in 10 mL of toluene produced a white suspension. This was stirred for 30 min and the white solid produced filtered off, washed with 5 mL of toluene and then dried *in vacuo*.

Observation of *trans*-[OsH(CNBF_3)(dppe)$_2$] 5Os2. *Method 1.* One equivalent of [$HPPh_3$]BF_4 was added to one equivalent of *trans*-[OsH(CN)(dppe)$_2$] in benzene or toluene. After stirring for 30 min the white complex **2*Os2** was isolated by decanting the solvent followed by washing with benzene or toluene and then drying under a vacuum. When it was dissolved in CD_2Cl_2 and left in solution for several days it started converting into **5Os2**.

Method 2. When one equivalent of $BF_3 \cdot Et_2O$ was added to a small amount of **2*Os2** in toluene a white precipitate formed which was isolated as in Method 1. The ^{1}H NMR spectrum revealed a mixture of three species: **2*Os2**, **3*Os2**,[5] and **5Os2**.

***trans*-[RuH(CNBF_3)(dppp)$_2$] 5Ru3.** *trans*-[Ru(η^2-H_2)(CNBF_3)(dppp)$_2$]BF_4 **7*Ru3** (0.29 g, 0.26 mmol) was dissolved in 15 mL of CH_2Cl_2. NEt_3 (56 μl, 0.40 mmol) was added and the solution stirred at room temperature for 10 minutes. Then, 20 mL of Pr^{i}OH were added and after concentration of the solution a white precipitate formed which was filtered off, washed with Pr^{i}OH, dried under a vacuum and then recrystallized from a CH_2Cl_2–Pr^{i}OH mixture.

***trans*-[OsH(CNBF_3)(dppp)$_2$] 5Os3.** *trans*-[Os(η^2-H_2)(CNBF_3)(dppp)$_2$]BF_4 **7*Os3** (0.20 g, 0.17 mmol) was dissolved in 10 mL of CH_2Cl_2. NEt_3 (33 μl, 0.24 mmol) was added and the solution stirred at room temperature for 10 minutes. Then, 10 mL of Pr^{i}OH were added and after concentration of the solution a white precipitate formed which was filtered off, washed with Pr^{i}OH, dried under a vacuum and then recrystallized from a CH_2Cl_2–Pr^{i}OH mixture.

***trans*-[RuH(CNBPh_3)(dppe)$_2$] 6Ru2.** *Method 1.* Crude *trans*-[RuH(CN)(dppe)$_2$] containing $KBPh_4$ (0.050 g, 0.054 mmol) was dissolved in 5 mL of benzene. [$HPPh_3$]BF_4 (0.014 g, 0.040 mmol) was added and stirred for 30 min. A white solid was obtained when the solvent was removed *in vacuo*. The NMR spectra (^{1}H and ^{31}P-{^{1}H}) of the product revealed a mixture of complexes **5Ru2** and **6Ru2**. Colourless crystals suitable for structure determination were obtained by slow evaporation of the solvent from a concentrated solution of the product in CH_2Cl_2.

Method 2. Triphenylboron (0.03 g, 0.12 mmol) was added to a solution of *trans*-[RuH(CN)(dppe)$_2$] (0.10 g, 0.11 mmol) in 10 mL of toluene and stirred for 30 min. A white solid was produced when the solvent was removed *in vacuo*.

[Ru(η^2-H_2)(CNBF_3)(dppp)$_2$]BF_4 7*Ru3. *trans*-[RuH(CN)(dppp)$_2$] (0.20 g, 0.21 mmol) was dissolved in 30 mL of C_6H_6 under H_2. Upon addition of 85% $HBF_4 \cdot Et_2O$ (91 mL, 0.53 mmol) a white precipitate was formed, that was filtered off, washed with C_6H_6, and dried in vacuum.

[Os(η^2-H_2)(CNBF_3)(dppp)$_2$]BF_4 7*Os3. *trans*-[OsH(CN)(dppp)$_2$] (0.20 g, 0.19 mmol) was dissolved in 30 mL of C_6H_6 under H_2. Upon addition of 85% of $HBF_4 \cdot Et_2O$ (82 mL, 0.48 mmol) a white precipitate was formed, which was filtered off, washed with C_6H_6, and dried in vacuum.

[Ru(FBF_3)(CNBF_3)(dppp)$_2$] 8Ru3. 7*Ru3 (0.30 g, 0.27 mmol) was dissolved in CH_2Cl_2 (20 mL) and argon bubbled at room

Table 7 Crystallographic data for complexes **2Ru2**, **2*Os2**, **5Ru2**, and **6Ru2**

	2Ru2	**2*Os2**	**5Ru2**·CH_2Cl_2	**6Ru2**·CH_2Cl_2
Empirical formula	$C_{54}H_{50}F_3NO_3P_4RuS$	$C_{53}H_{50}BF_4NOsP_4$	$C_{54}H_{51}BCl_2F_3NP_4Ru$	$C_{72}H_{66}BCl_2NP_4Ru$
Formula weight	1074.96	1101.83	1077.62	1251.9
T/K	173(1)	173(2)	173(2)	173(2)
Crystal system	Monoclinic	Monoclinic	Monoclinic	Monoclinic
Space group	$P2_1/n$	$P2_1/n$	$P2_1/n$	$P2_1/c$
a/Å	16.536(4)	12.825(2)	12.254(2)	14.977(1)
b/Å	17.005(2)	21.230(3)	22.046(3)	22.955(3)
c/Å	22.280(8)	18.373(2)	19.251(2)	18.864(3)
β/°	96.73(2)	107.90(1)	108.16(1)	108.86(1)
V/Å³	6222(3)	4760(1)	4942(1)	6137(1)
Z	4	4	4	4
μ/mm^{-1}	0.433	2.867	0.605	0.491
Reflections collected	9532	10732	12465	13869
Independent reflections	9202	10286	11926	13363
Final *R*1, *wR*2 [$I > 2\sigma(I)$]	0.046, 0.126	0.044, 0.096	0.040, 0.100	0.033, 0.067
(all data)	0.059, 0.132	0.076, 0.103	0.056, 0.105	0.056, 0.071

temperature for 30 min. Addition of hexane (20 mL) and concentration gave a white precipitate. The crude white product was dried in vacuum and recrystallized from CH_2Cl_2–hexane.

Single crystal structure determinations

Data on crystals of complexes **5Ru2**, **6Ru2**, **2Ru2** and **2*Os2** were collected by use of a Siemens P4 diffractometer and Mo-Kα radiation ($\lambda = 0.71073$ Å). Crystallographic details are summarized in Table 7. The structures were solved and refined using the SHELXTL PC V5.1 package.[47] All non-hydrogen atoms were refined with anisotropic thermal parameters to minimize $\Sigma w(F_o - F_c)^2$. Hydrogen atoms were included in calculated positions and treated as riding atoms. The positions of the hydride atoms were determined from difference electron density maps and refined with isotropic thermal parameters.

CCDC reference number 186/2170.

See http://www.rsc.org/suppdata/dt/b0/b005687l/ for crystallographic files in .cif format.

Acknowledgements

We thank NSERC for a grant to R. H. M., DAAD for grants to T. S. and Patrick Amrhein who did preliminary experiments and Johnson-Matthey PLC for a loan of ruthenium salts. Consiglio Nazionale delle Ricerche and Ministero dell'Università e della Ricerca Scientifica e Tecnologica are gratefully acknowledged. The Regione Autonoma FVG (Italy) is also acknowledged for a grant to E. R.

References

1 W. P. Fehlhammer and M. Fritz, *Chem. Rev.*, 1993, **93**, 1243.
2 P. I. Amrhein, S. D. Drouin, C. E. Forde, A. J. Lough and R. H. Morris, *Chem. Commun.*, 1996, 1665.
3 T. P. Fong, A. J. Lough, R. H. Morris, A. Mezzetti, E. Rocchini and P. Rigo, *J. Chem. Soc.*, *Dalton Trans.*, 1998, 2111.
4 C. E. Forde, S. E. Landau and R. H. Morris, *J. Chem. Soc.*, *Dalton Trans.*, 1997, 1663.
5 T. P. Fong, C. E. Forde, A. J. Lough, R. H. Morris, P. Rigo, E. Rocchini and T. Stephan, *J. Chem. Soc.*, *Dalton Trans.*, 1999, 4475.
6 C. Nataro, J. B. Chen and R. J. Angelici, *Inorg. Chem.*, 1998, **37**, 1868.
7 S. S. P. R. Almeida, M. F. C. Guedes da Silva, J. J. R. Fraústo da Silva and A. J. L. Pombeiro, *J. Chem. Soc.*, *Dalton Trans.*, 1999, 467.
8 D. S. Frohnapfel, S. Reinartz, P. S. White and J. L. Templeton, *Organometallics*, 1998, **17**, 3759.
9 A. J. L. Pombeiro, D. L. Hughes, C. J. Pickett and R. L. Richards, *J. Chem. Soc.*, *Chem. Commun.*, 1986, 246.
10 L. A. Cardoza and R. J. Angelici, *Inorg. Chem.*, 1999, **38**, 1708.
11 M. F. N. N. Carvalho, M. T. Duarte, A. M. Galvao, A. J. L. Pombeiro, R. Henderson, H. Fuess and I. Svoboda, *J. Organomet. Chem.*, 1999, **583**, 56.
12 K. H. Trylus, A. Schroder, I. Brudgam, R. Thiel and W. P. Fehlhammer, *Inorg. Chim. Acta*, 1998, **269**, 23.
13 E. Bar and W. P. Fehlhammer, *J. Organomet. Chem.*, 1988, **353**, 197.
14 W. Weigand, U. Nagel and W. Beck, *J. Organomet. Chem.*, 1988, **352**, 191.
15 P. I. Amrhein, A. J. Lough and R. H. Morris, *Inorg. Chem.*, 1996, **35**, 4523.
16 H. Vahrenkamp, A. Geiss and G. N. Richardson, *J. Chem. Soc.*, *Dalton Trans.*, 1997, 3643.
17 R. L. Richards, *Coord. Chem. Rev.*, 1996, **154**, 83.
18 A. Volbeda, E. Garcin, C. Piras, A. L. De Lacey, V. M. Fernandez, E. C. Hatchikian, M. Frey and J. C. Fontecilla-Camps, *J. Am. Chem. Soc.*, 1996, **118**, 12989.
19 Y. Montet, E. Garcin, A. Volbeda, C. Hatchikian, M. Frey and J. C. Fontecilla-Camps, *Pure Appl. Chem.*, 1998, **70**, 25.
20 A. J. Pierik, W. Roseboom, R. P. Happe, K. A. Bagley and S. P. J. Albracht, *J. Biol. Chem.*, 1999, **274**, 3331.
21 E. J. Lyon, I. P. Georgakaki, J. H. Reibenspies and M. Y. Darensbourg, *Angew. Chem.*, *Int. Ed.*, 1999, **38**, 3178.
22 K. K. Klausmeyer, S. R. Wilson and T. B. Rauchfuss, *J. Am. Chem. Soc.*, 1999, **121**, 2705.
23 S. M. Holmes and G. S. Girolami, *J. Am. Chem. Soc.*, 1999, **121**, 5593.
24 F. A. Cotton, G. Wilkinson, C. A. Murillo and M. Bochmann, *Advanced Inorganic Chemistry*, Wiley, New York, 1999.
25 S. D. Ittel, C. A. Tolman, P. J. Krusic, A. D. English and J. P. Jesson, *Inorg. Chem.*, 1978, **17**, 3432.
26 J. Chatt and R. G. Hayter, *J. Chem. Soc.*, 1961, 2605.
27 S. D. Ittel, C. A. Tolman, A. D. English and J. P. Jesson, *J. Am. Chem. Soc.*, 1978, **100**, 7577.
28 V. N. Sapunov, K. Mereiter, R. Schmid and K. Kirchner, *J. Organomet. Chem.*, 1997, **530**, 105.
29 K. M. Mackay and R. A. Mackay, *Introduction to Modern Inorganic Chemistry*, Prentice Hall, Englewood Cliffs, NJ, 1989.
30 C. J. Pouchert, *The Aldrich Library of Infrared Spectra*, Aldrich Chemical Company Inc., Milwaukee, WI, 1975.
31 Z. Dega-Szafran and M. Szafran, *J. Chem. Soc.*, *Perkin Trans. 2*, 1982, 195.
32 Z. Dega-Szafran, E. Dulewicz and M. Szafran, *J. Chem. Soc.*, *Perkin Trans. 2*, 1984, 1997.
33 A. Filarowski and A. Koll, *Vib. Spectrosc.*, 1996, **12**, 15.
34 T. P. Hanusa and D. J. Burkey, in *Encyclopedia of Inorganic Chemistry*, John Wiley & Sons Ltd., Chichester, 1994.
35 R. H. Morris and R. Wittebort, *Magn. Reson. Chem.*, 1997, **35**, 243.
36 P. A. Maltby, M. Schlaf, M. Steinbeck, A. J. Lough, R. H. Morris, W. T. Klooster, T. F. Koetzle and R. C. Srivastava, *J. Am. Chem. Soc.*, 1996, **118**, 5396.
37 M. A. N. D. A. Lemos and A. J. L. Pombeiro, *J. Organomet. Chem.*, 1992, **438**, 159.
38 M. T. Bautista, E. P. Cappellani, S. D. Drouin, R. H. Morris, C. T. Schweitzer, A. Sella and J. D. Zubkowski, *J. Am. Chem. Soc.*, 1991, **113**, 4876.
39 J. Chatt, W. Hussain, G. J. Leigh, H. Mohd. Ali, C. J. Pickett and D. A. Rankin, *J. Chem. Soc.*, *Dalton Trans.*, 1985, 1131.
40 G. Jia and R. H. Morris, *J. Am. Chem. Soc.*, 1991, **113**, 875.
41 E. P. Cappellani, S. D. Drouin, G. Jia, P. A. Maltby, R. H. Morris and C. T. Schweitzer, *J. Am. Chem. Soc.*, 1994, **116**, 3375.

42 M. T. Bautista, K. A. Earl, P. A. Maltby, R. H. Morris, C. T. Schweitzer and A. Stella, *J. Am. Chem. Soc.*, 1988, **110**, 7031.
43 M. Aresta, P. Giannoccaro, M. Rossi and A. Sacco, *Inorg. Chim. Acta*, 1971, **5**, 115.
44 B. R. James and D. K. W. Wang, *Inorg. Chim. Acta*, 1976, **19**, L17.
45 E. Rocchini, A. Mezzetti, H. Rüegger, U. Burckhardt, V. Gramlich, A. Del Zotto, P. Martinuzzi and P. Rigo, *Inorg. Chem.*, 1997, **36**, 711.
46 G. M. Bancroft, M. J. Mays, B. E. Prater and F. P. Stefanini, *J. Chem. Soc. A*, 1970, 2146.
47 G. M. Sheldrick, SHELXTL PC V5.1, Bruker Analytical X-ray Systems, Madison, WI, 1997.